STM JOURNALS

Journal of
Polymer & Composites

ISSN: 2321-2810 (Online)
ISSN: 2321-8525 (Print)
Volume 11, Special Issue 7, 2023
DOI (Journal): 10.37591/JoPC

http://engineeringjournals.stmjournals.in/index.php/JoPC/index

Research JoPC

Breakup Fusion of ^{18}O with ^{144}Sm

Rajesh K. Sahoo[1], Dharmendra Singh[2,*], Amritraj Mahato[1], Nitin Sharma[1], Jagatjyoti Mohapatra[1], Lupteindu Chhura[1], Rahul Mahato[1], Pankaj K. Giri[3], Sneha B. Linda[1], Harish Kumar[4], Suhail A. Tali[4], Asif Ali[4], Rahbar Ali[5], S. Kumar[6], Nabendu K. Deb[7], N.P.M. Sathik[8], M. Afzal Ansari[9], R. Kumar[10], S. Muralithar[11], R.P. Singh[12]

Abstract

Excitation function measurements have been done for the evaporation residues populating in the system $^{18}O+^{144}Sm$. For this purpose, the stacked foil activation technique has been used subsequently accompanied by offline γ-ray spectrometry. The analysis of the experimental cross section of three evaporation residues $^{158}Tm(p3n)$, $^{157}Tm(p4n)$, and $^{155}Ho(ap2n)$ has been done in the light of theoretical code PACE-4. Current findings demonstrate that the experimental cross sections of evaporation residues formed via xn and pxn-emission channels follow the PACE-4 predictions, confirming that these evaporation residues are produced exclusively by complete fusion. Similarly, the cross sections of the evaporation residues generated via α-emission pathways exhibit notable enhancement in contrast to the code predictions. The increase in cross sections seen can be credited to the fragmentation of the projectile ^{18}O resulting in incomplete fusion. It has also been observed that there is a likelihood for the projectile to experience fragmentation i.e., ^{18}O into $^{14}C+$ α increases as the energy of the projectile increases.

***Author for Correspondence**
Dharmendra Singh
E-mail: dsinghcuj@gmail.com

[1]Research Scholar, Department of Physics, Central University of Jharkhand, Ranchi, India
[2]Associate Professor and Head, Department of Physics, Central University of Jharkhand, Ranchi, India
[3]Research Associate, UGC-DAE Consortium for Scientific Research, Kolkata Center, Kolkata, India
[4]Research Scholar, Department of Physics, Aligarh Muslim University, Aligarh, India
[5]Associate Professor, Department of Physics, G. F. (P. G.) College, Shahjahanpur, India
[6]Research Scholar, Nuclear Physics Group, Inter University Accelerator Centre, Aruna Asaf Ali Marg, New Delhi, India
[7]Research Scholar, Department of Physics, Gauhati University, Guwahati, Assam, India
[8]Associate Professor, Department of Physics, Jamal Mohamed College, Tiruchirappalli, India
[9](Retd.) Professor, Department of Physics, Aligarh Muslim University, Aligarh, India
[10]Scientist-F, Nuclear Physics Group, Inter University Accelerator Center, Aruna Asaf Ali Marg, New Delhi, India
[11]Scientist-H, Nuclear Physics Group, Inter University Accelerator Center, Aruna Asaf Ali Marg, New Delhi, India
[12]Scientist-G, Nuclear Physics Group, Inter University Accelerator Center, Aruna Asaf Ali Marg, New Delhi, India

Received Date: August 14, 2023
Accepted Date: August 31, 2023
Published Date: September 12, 2023

Citation: Rajesh K. Sahoo, Dharmendra Singh, Amritraj Mahato, Nitin Sharma, Jagatjyoti Mohapatra, Lupteindu Chhura, Rahul Mahato, Pankaj K. Giri, Sneha B. Linda, Harish Kumar, Suhail A. Tali, Asif Ali, Rahbar Ali, S. Kumar, Nabendu K. Deb, N.P.M. Sathik, M. Afzal Ansari, R. Kumar, S. Muralithar, R.P. Singh. Breakup Fusion of ^{18}O with ^{144}Sm. Journal of Polymer & Composites. 2023; 11(Special Issue 7): S53–S59.

Keywords: Heavy ion, Coulomb barrier, CF and ICF, CCFULL, PACE-4

INTRODUCTION

It has always been a primary focus of research to extensively examine the Heavy Ion (HI) produced fusion reaction [1] because it facilitates research into the properties of nuclei far from the β-stability line. In a nuclear fusion reaction, when the energy of the projectile exceeds the coulomb barrier of the system then complete fusion (CF) is anticipated to be the dominant reaction. However, recent investigations [1–3] show the distinct contribution of the incomplete fusion (ICF) phenomena. During the CF process, the projectile and the target nucleus merge completely, resulting in the formation of an energized compound nucleus (CN). The projectile transfers all of its momentum to the target. In contrast, the projectile disintegrates into its fragment parts in ICF. While one fragment moves ahead at almost the same speed, another fragment fuses with the target nucleus to form an

incompletely fused composite system. A fraction of momentum is transferred from the projectile to the composite system.

In comparison to CF, these ICF fragments have higher angular momenta but a lower excitation energy and mass/charge. Figure 1 shows the CF and ICF process. Experimental evidence for such types of measurements using projectile ^{12}C, ^{16}O, and ^{14}N with targets ^{197}Au and ^{209}Bi was reported [4]. Further, Inamura et al. [5] furnished the significant information related to ICF. In theoretical aspects, several models of ICF were also proposed but none of the theoretical models has been able to predict the dynamics governing ICF reactions occurring at projectile energy lower than 10 MeV/nucleon. The SUMRULE model was suggested [6] to interpret the impact of input angular momentum in CF and ICF reactions. According to the SUMRULE model, ICF arises from peripheral interactions and has a major contribution to the total fusion (TF) in ℓ space above ℓ_{crit} where effective potential disperses and consequently, the capturing probability of the projectile by the target nuclei gets impeded. Gerschel et al. [7] found that the target deformation was affecting the localization of ℓ window. Recent studies are [1–3,8] also evident that the ICF dynamics depend on different entrance channel parameters rather than a single parameter.

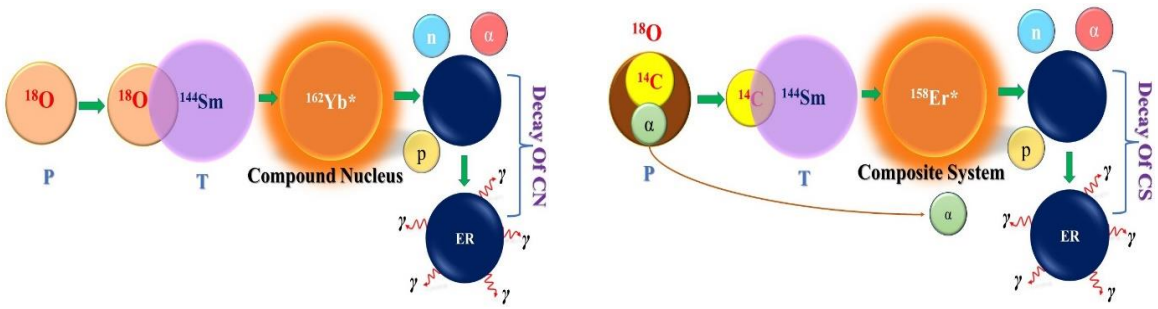

Figure 1. Pictorial Representation of Complete and Incomplete Fusion.

The current work involves measuring the excitation functions (EFs) of the evaporation residues (ERs) produced in the ^{18}O+^{144}Sm system at a beam energy (E_{lab}) range of 4-6MeV/A. The PACE-4 has been utilized for theoretical predictions to analyse the data [9].

DETAILS OF THE EXPERIMENTAL TECHNIQUE

The EFs experiment was carried out by utilizing a 15UD accelerator of tandem type at the Inter-University Accelerator Centre (IUAC), New Delhi, India. In these particular measurements, the stacked foil activation method was employed through offline γ-ray measurements. Isotopically enriched ^{144}Sm target (thickness∼250-550 μg/cm^2) with enrichment ≈ 97.63% were deposited on thick aluminium (^{27}Al) foils ≈ 0.7-1.7 mg/cm^{2}thickness at the target fabrication lab, IUAC (Figure 2). The fabricated targets were adhered to stainless steel (SS) holders with concentric holes that were 1 cm in diameter. SS holders are also covered in a silver colloid paste for quick heat dissipation during the experiment. A single stack containing seven ^{144}Sm targets along with ^{27}Al catcher foils was irradiated with $^{18}O^{7+}$ ion beam having energy 103 MeV in the GPSC chamber at IUAC as shown in Figure 2. The arrangement of the ^{144}Sm stack was such that the ^{144}Sm target was facing the ^{18}O beam. After the irradiation, the populated residue got trapped in successive ^{27}Al catcher foils. Keeping in mind the decay time of populated residues, the ^{18}O beam was incident on the ^{144}Sm target stack for ≈10 hours. The Charge collector was employed to measure the beam current during these experiments and found to be ∼ 1-2 pnA. The SRIM-2008 [10] software was used to calculate the energy degradation at each foil of the stack. After the irradiation, induced γ activities of the trapped ERs in the ^{27}Al catcher foils were detected by HPGe detectors of known efficiency with CANDLE software [11]. The detector was precalibrated by using a standard ^{152}Eu ($T_{1/2}$ =13.517 yr) source. The HPGe detector utilized in the present experiment had a peak resolution ≈ 2.0 KeV. The energy of γ-ray, branching ratios (θ), half-lives of ERs, etc were taken from the Table of Isotopes [12]. The ERs populated via CF and ICF reaction channels in the

$^{18}O+^{144}Sm$ system are $^{158}Tm(p3n)$, $^{157}Tm(p4n)$, and $^{155}Ho(\alpha p2n)$. The identification of these ERs was based on their characteristic γ-rays and subsequent confirmation of their half-lives. A standard calibrated γ-spectrum for the system $^{18}O+^{144}Sm$ at projectile energy ≈103 MeV is displayed in Figure 3. The half-life plot for ER ^{158}Tm ($T_{1/2}$= 3.98 min), ^{157} Tm ($T_{1/2}$=3.63 min), and ^{155}Ho ($T_{1/2}$= 48 min) are shown in Figure 4(a), (b) and (c). From the measured yields of each γ-ray, the cross sections were calculated using the standard formulation [13].

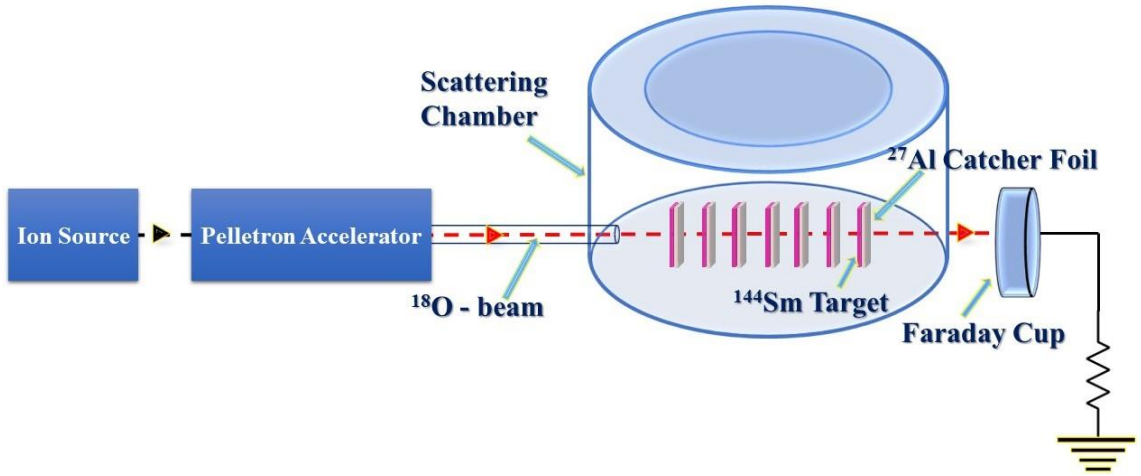

Figure 2. A Pictorial Representation of the Experimental setup.

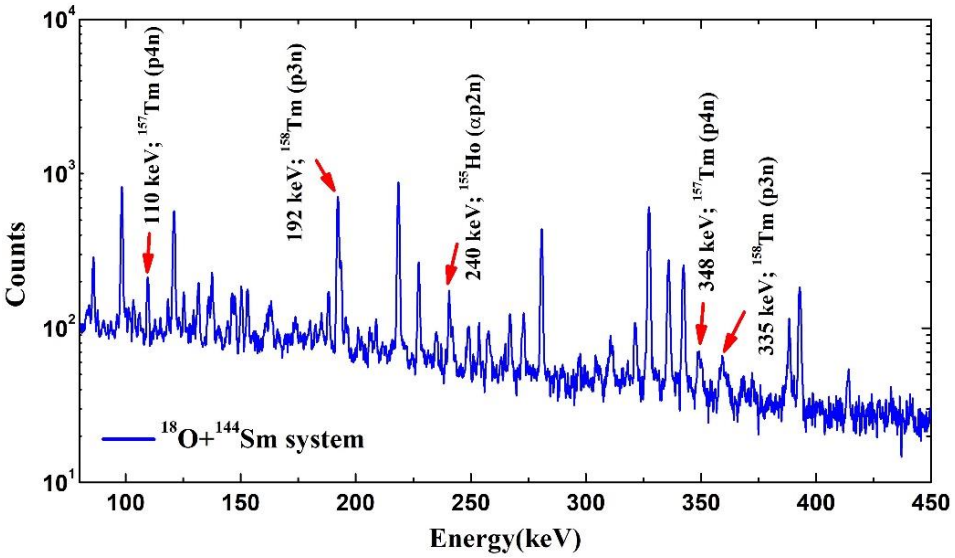

Figure 3. γ -ray energy spectra of the $^{18}O+^{144}Sm$ system at E_{lab} ≈ 103 MeV.

$$\sigma_{ER}(E) = \frac{A\lambda[\exp(-\lambda t_2)]}{N_0\phi\epsilon_G\theta C\,[1-\exp(-\lambda t_1)][1-\exp(-\lambda t_3)]} \quad (1)$$

Here A represents an area under the photo peak, λ represents the disintegration constant of the ER, N_0 refers to the areal density of target nuclei, ϕ represents the incident ion beam flux, ϵ_G represents the geometry-dependent efficiency, θ represents the branching ratio of the distinct γ-ray signature. C = [1-exp (-μd)] self-absorption correction factor. The aspects which can be responsible for errors and uncertainty in the experimental cross sections like (i) beam current fluctuation, (ii) uncertainty due to the error in target measurements, (iii) error in the calibration of detector's efficiency, were also considered, and hence cross sectional measurements experienced margins of error corresponding to percentages 6%, 3% and 5% respectively.

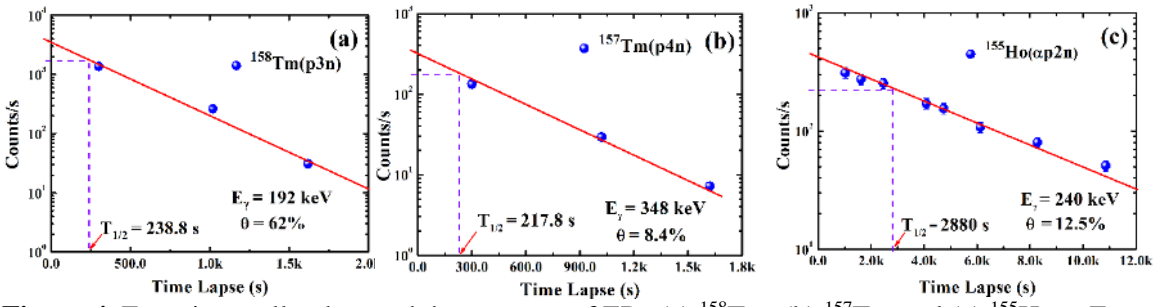

Figure 4. Experimentally observed decay curve of ERs (a) ^{158}Tm, (b) ^{157}Tm and (c) ^{155}Ho at $E_{lab} \approx 103$ MeV populated in ^{18}O+^{144}Sm system.

RESULTS AND DISCUSSION

In the current work, EFs of the ERs ^{158}Tm(p3n), ^{157}Tm(p4n), and ^{155}Ho(αp2n) produced in the interaction of ^{18}O with ^{144}Sm via CF and ICF channels were measured. Theoretical calculations of EFs for these residues were done by employing the standard statistical code PACE-4. Due to very short half-life ERs produced via xn reaction channels were unable to be identified during decay curve analysis. During the decay curve analysis, two ERs ^{158}Tm(p3n) and ^{157}Tm(p4n) involving precursor contribution from ^{158}Yb(5n) and ^{157}Yb(6n) respectively have been observed. Cross section of ERs ^{158}Tm with a half-life of 3.98 min was observed to be significantly populating from its precursor isobar ^{158}Yb which has a very short half-life of 1.49 min. Similarly, cross section of ERs ^{157}Tm with a half-life of 3.63 min was observed to be significantly fed from its precursor ^{157}Yb having a very short half-life of 38.6 sec. Due to a very short half-life, the experimental cross section of ^{158}Yb and ^{157}Yb could not be determined. The independent cross sections (σ_{indp}) of ^{158}Tm and ^{157}Tm were derived using standard formulations [14] given by

$$F_{pre} = P_{pre} \frac{t_{1/2}^{d}}{(t_{1/2}^{d} - t_{1/2}^{pre})} \tag{2}$$

$$\sigma_{indp} = \sigma_{cuml} - F_{pre}\sigma_{pre} \tag{3}$$

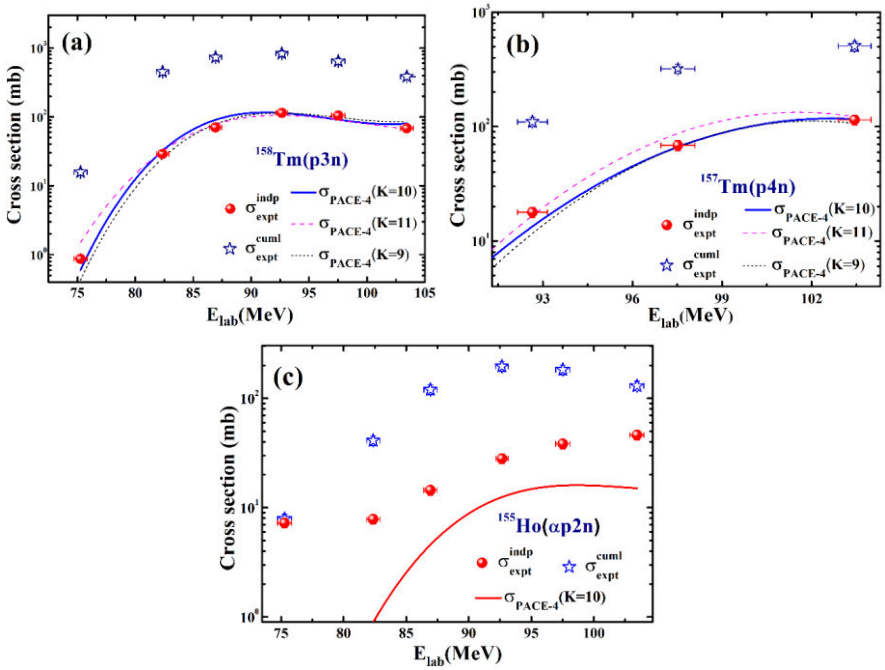

Figure 5. EFs of ERs (a) ^{158}Tm(p3n), (b) ^{157}Tm(p4n) and c) ^{155}Ho(αp2n) populated via pxn and αpxn in the system ^{18}O+^{144}Sm with theoretical projections of PACE-4.

Within the provided equation, P_{pre} represents the fraction of decay branching from the precursor to its daughter nuclei. The quantities $t_{1/2}^{d}$ and $t_{1/2}^{pre}$ stand for the half-lives of the daughter and precursor nuclei, respectively. The numerical values of the half-lives and the branching ratio (θ) of the precursor decay (P_{pre}) are extracted from the ref. [12]. Therefore, the independent cross sections of ERs ^{158}Tm and ^{157}Tm were extracted from their cumulative cross section using the given formula:

$$\sigma_{indp}^{158Tm} = \sigma_{cuml}^{158\mathrm{Tm}} - 1.598\,\sigma_{PACE}^{158Yb} \quad (4)$$

$$\sigma_{indp}^{157Tm} = \sigma_{cuml}^{157\mathrm{Tm}} - 1.209\,\sigma_{PACE}^{157Yb} \quad (5)$$

During analysis, the experimental cross section of ERs ^{155}Er(α3n) with a half-life of 48 min is anticipated to act as a precursor for ^{155}Ho(αp2n) but could not be determined due to the absence of its characteristicsγ line in the literature. Therefore, the theoretically predicted cross section by PACE- 4 was used for calculating the independent cross section of ^{155}Ho using the formulation:

$$\sigma_{indp}^{155Ho} = \sigma_{cuml}^{155\mathrm{Ho}} - 1.121\,\sigma_{PACE}^{155Er} \quad (6)$$

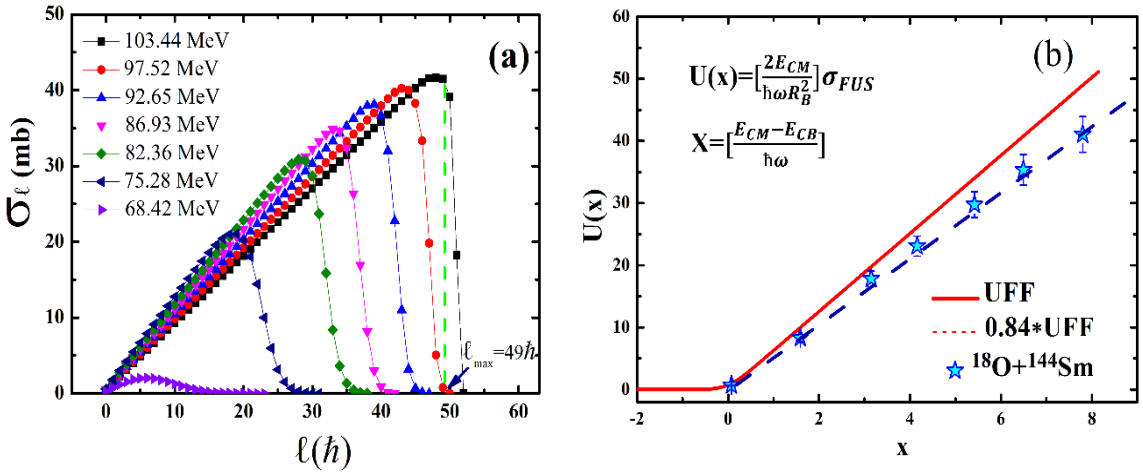

Figure 6. (a) Fusion ℓ-distributions calculated using CCFULL code for thesystem ^{18}O+^{144}Sm (b) The measured fusion functions (MFFs) with UFF for the ^{18}O+^{144}Sm system.

The measured independent cross section of the ERs populated via pxn channels were plotted as a function of projectile energy, alongside PACE-4 predictions with different level density parameter constant K= 9,10, and 11 as shown in Figure 5 (a) and (b). It can be observed from Figure 5(a) and (b) that the measured independent cross section of ^{158}Tm(p3n) and ^{157}Tm(p4n) agree well with the PACE-4 predictions with level density parameter constant K=10. Therefore, these ERs are produced in the CF process only. Further, from Figure 5 (c) the ERs ^{155}Ho shows a significant enhancement over PACE- 4 predictions at K=10. Since the PACE-4 predictions do not include the ICF process for the cross section calculation, therefore any rise in experimental cross section than theoretical prediction is ascribed that the ER not only populated via CF but also populated via the ICF process. Further, an attempt has been made to study the fusion ℓ distribution of the ^{18}O+^{144}Sm system using the code CCFULL [15]. It is important to mention that the CCFULL code's calculations do not take into account the interaction with unbound or continuum states or the impact of projectile breakup. Figure 6(a) represents the fusion ℓ distribution for the system ^{18}O+^{144}Sm at different projectile energies. As can be seen from Figure 6(a) ℓ_{max} corresponding to the highest energy is found to be ≈ 49ħ. To further strengthen the existing findings, the present system ^{18}O+^{144}Sm was also analyzed under the reduction procedure of universal fusion function (UFF) [16]. This procedure serves to remove the geometric and static influences originating from the potential acting between the interacting partners. Therefore, any discrepancies between the measured fusion function (MFFs) and the UFF can be attributed to the impact of the projectile's breakup

phenomenon. The measured CF cross section has been reduced using this prescription plotted with UFF as shown in Figure 6 (b). The input parameters used for UFF calculations were taken as Coulomb Barrier (E_{CB}) = 60.85 MeV, Barrier Radius (R_B) = 11.35 fm, and Barrier Curvature ($\hbar\omega$) = 4.02 MeV. It is evident from this illustration that the reduced CF cross section is suppressed by ≈ 16% than UFF. Consequently, the divergence observed in the Measured Fusion Functions compared to the UFF can be ascribed to the breakup of the ^{18}O projectile into $^{14}C+\alpha$.

CONCLUSION

The identification of the ERs ^{158}Tm, ^{157}Tm, and ^{155}Ho populated in the $^{18}O+^{144}Sm$ system has been done in the energy regime of ≈ 4-6 MeV/A. The EFs of ERs ^{158}Tm and ^{157}Tm were compared with PACE-4, after deducing the independent cross section from their precursor contributions. The measured EFs of the ERs ^{158}Tm and ^{157}Tm were found to be in good agreement with theoretical predictions, proving that these ERs are exclusively produced by the CF process. On the other hand, the ER ^{155}Ho populated through the α emission channel shows significant enhancement from their theoretical predictions. The enhanced cross section signifies the population of this residue via CF and /or ICF. The contribution of ICF is observed because ^{18}O breaks up into $\alpha + ^{14}C$.

Acknowledgment

The authors acknowledge the support from the Director and Pelletron operating staff of IUAC, New Delhi. The authors also acknowledgethe support from in charge of the Target lab and Mr. Abhilash S.R. during target preparation, Head, Department of Physics, Central University of Jharkhand, Ranchi for his motivation and assistance.

REFERENCES

1. Mahato A, Singh D, Sharma N, et al. Effects of entrance channels on breakup fusion induced by F 19 projectiles. Physical Review C. 2022 Jul 19;106(1):014613.
2. Mahato A, Singh D, Giri PK, et al. Probing of incomplete fusion dynamics in N 14+ Sn 124 system and its correlation with various entrance channel effects. The European Physical Journal A. 2020 May; 56:1-5.
3. Giri PK, Singh D, Mahato A, et al. Systematic study of low-energy incomplete-fusion dynamics in the O 16 + Nd 148 system: Role of target deformation. Physical Review C. 2019 Aug 22;100(2):024621.
4. Britt HC, Quinton AR. Alpha particles and protons emitted in the bombardment of Au 197 and Bi 209 by C 12, N 14, and O 16 projectiles. Physical Review. 1961 Nov 1;124(3):877.
5. Inamura T, Ishihara M, Fukuda T, et al. Gamma-rays from an incomplete fusion reaction induced by 95 MeV 14N. Physics Letters B. 1977 May 9;68(1):51-4.
6. Wilczynski J, Siwek-Wilczynska K, Van Driel J, et al. Incomplete fusion reactions in N 14+Tb 159 system and a "sum-rule model" for fusion and incomplete fusion reactions. Phys. Rev. Lett.;(United States). 1980 Aug 25;45(8).
7. Gerschel C. Proc. Int. Conf. on selected aspects of heavy ion reactions. In Nucl. Phys. 1982 (Vol. 387, p. 297c). North-Holland Amsterdam.
8. Singh D, Linda SB, Giri PK, et al. Role of input angular momentum and target deformation on the incomplete-fusion dynamics in the O 16+ Sm 154 system at E_{Lab} = 6.1 MeV/nucleon. Physical Review C. 2018 Jun 7;97(6):064604.
9. Gavron A. Statistical model calculations in heavy ion reactions. Physical Review C. 1980 Jan 1;21(1):230.
10. JP ZJ. SRIM-The stopping and range of ions in matter. Nucl. Instrum. Methods Phys. Res., Sect. B. 2010;268(11-12):1818-23.
11. E. T. Subramaniam, B. P. Ajith Kumar, R. K. Bhowmik, http://www.iuac.res.in/NIAS.
12. National Nuclear Data Center, Brookhaven National Laboratory https://www.nndc.bnl.gov/nudat3/
13. Ansari MA, Singh RK, Sehgal ML, et al. Isomeric cross-sections of In and Rh at neutron energies of a few MeV. Annals of Nuclear Energy. 1984 Jan 1;11(12):607-9.

14. Cavinato M, Fabrici E, Gadioli E, et al. Study of the reactions occurring in the fusion of C 12 and O 16 with heavy nuclei at incident energies below 10 MeV/nucleon. Physical Review C. 1995 Nov 1;52(5):2577.
15. Hagino K, Rowley N, Kruppa AT. A program for coupled-channel calculations with all order couplings for heavy-ion fusion reactions. Computer Physics Communications. 1999 Dec 1;123(1-3):143-52.
16. Canto LF, Junior DM, Gomes PR, et al. Reduction of fusion and reaction cross sections at near-barrier energies. Physical Review C. 2015 Jul 29;92(1):014626.

